Electronic Supplementary Material (ESI) for Journal of Materials Chemistry B.

Supporting Information for

Bifunctional MIL-53(Fe) with pyrophosphate-mediated peroxidase-like activity and oxidation-stimulated fluorescence switching for alkaline phosphatase detection

Kun Ye,[a] Linjie Wang,[a] Hongwei Song,[b] Xin Li,[a] Xiangheng Niu[a,*]

[a] Institute of Green Chemistry and Chemical Technology, School of Chemistry and Chemical Engineering, Jiangsu University, Zhenjiang 212013, China

[b] School of Environmental and Chemical Engineering, Jiangsu University of Science and Technology, Zhenjiang 212003, China

* Corresponding author. E-mail: niuxiangheng@126.com

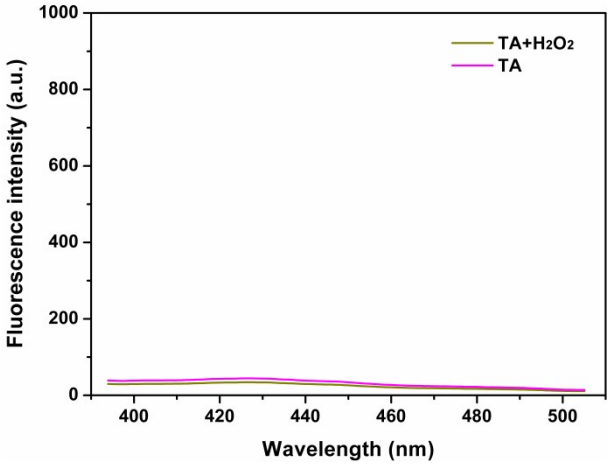

Figure S1. Fluorescence spectra of TA and TA+H_2O_2.

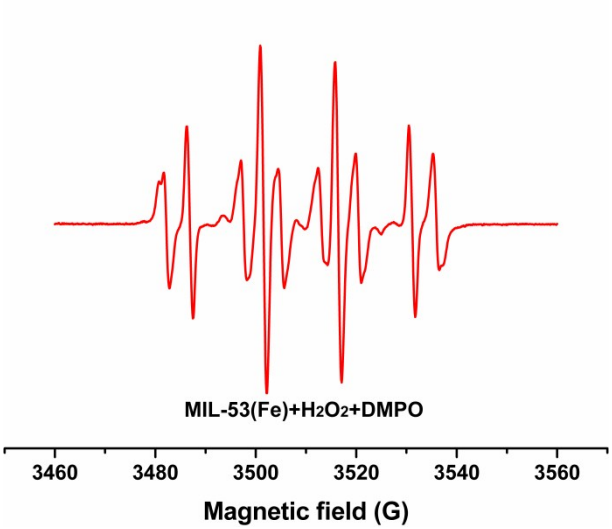

Figure S2. EPR spectrum of the MIL-53(Fe)+H_2O_2+DMPO system.

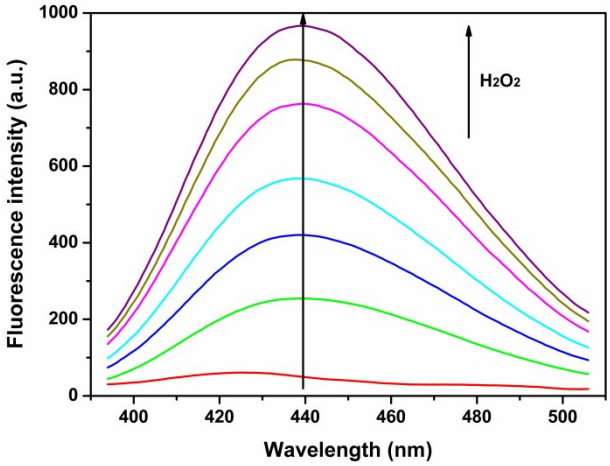

Figure S3. Fluorescence spectra of the MIL-53(Fe)+H_2O_2 system with different

concentrations of H_2O_2.

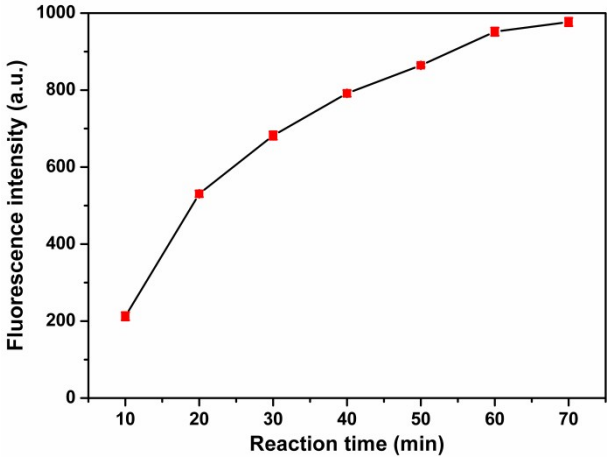

Figure S4. Fluorescence intensity of the MIL-53(Fe)+H_2O_2 system upon reaction time.

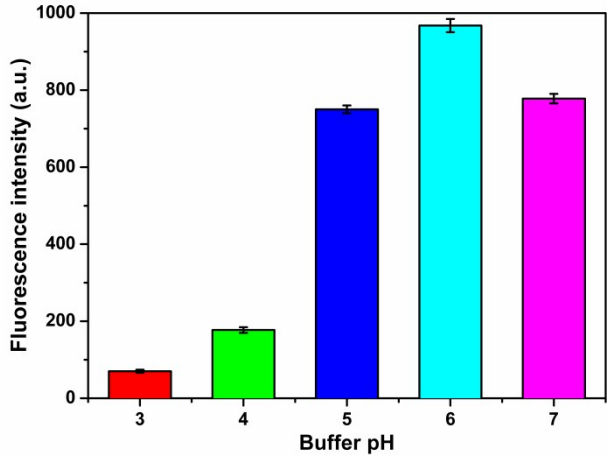

Figure S5. Effect of buffer pH on the fluorescence intensity of the MIL-53(Fe)+H_2O_2 system.

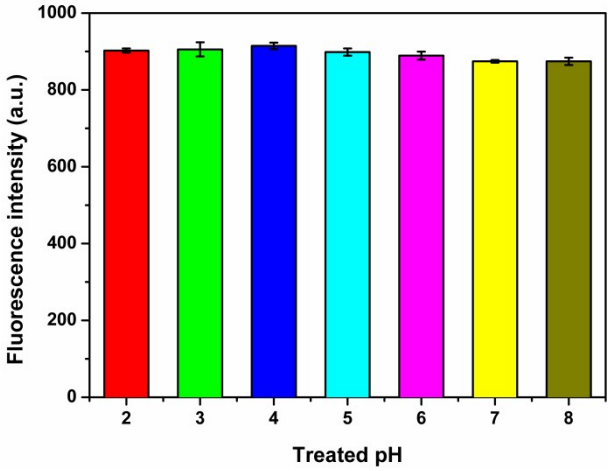

Figure S6. Robustness of the synthesized MIL-53(Fe) against harsh pH. The material was first treated by incubating it in 0.1 M buffers with different pH for 2 h, and then its oxidation-stimulated fluorescence was measured under standard conditions.

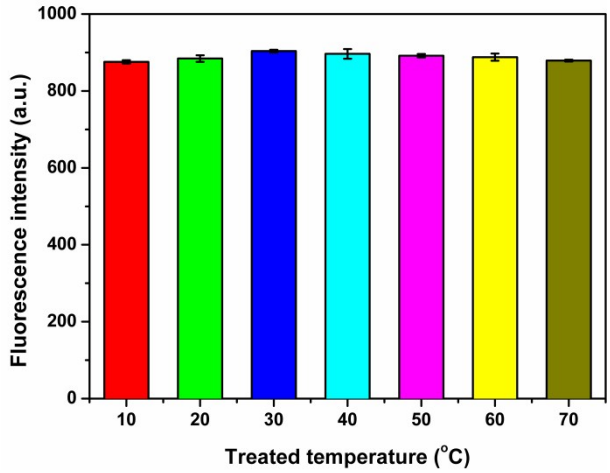

Figure S7. Robustness of the synthesized MIL-53(Fe) against harsh temperature. The material was first treated by incubating it at different temperatures for 2 h, and then its oxidation-stimulated fluorescence was measured under standard conditions.

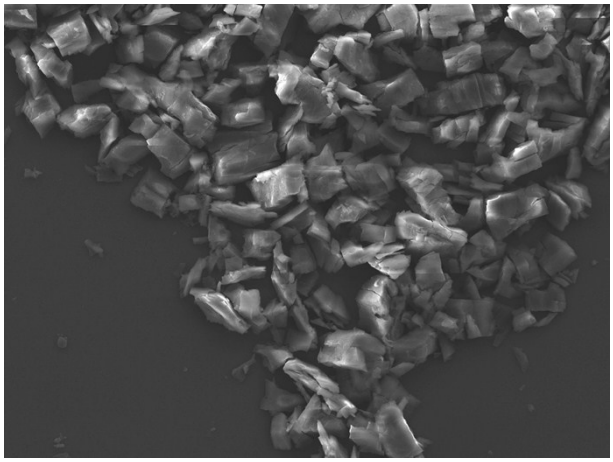

Figure S8. SEM image of the PPi-capped MIL-53(Fe).

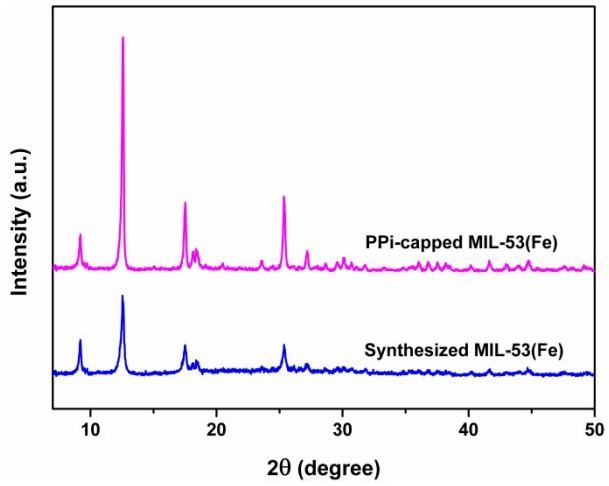

Figure S9. Comparison of XRD patterns of MIL-53(Fe) and PPi-capped MIL-53(Fe).

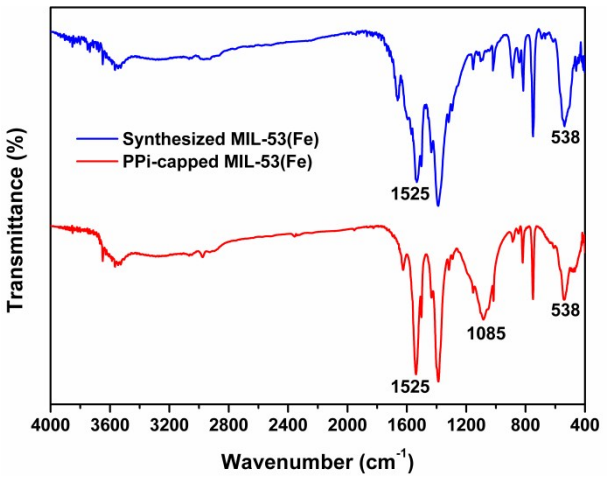

Figure S10. Comparison of FTIR spectra of MIL-53(Fe) and PPi-capped MIL-53(Fe).

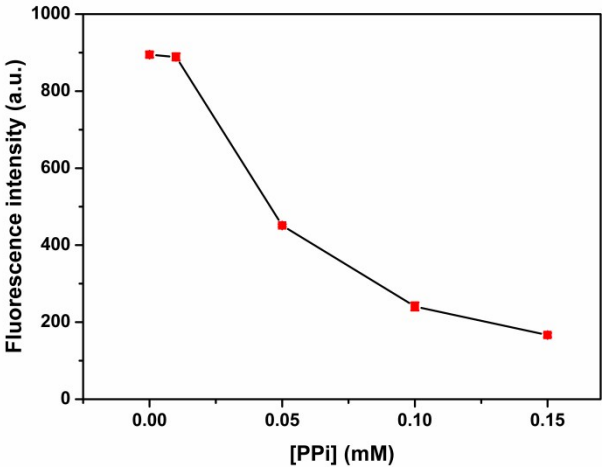

Figure S11. Effect of PPi concentration on the inhibition of the MIL-53(Fe)+H_2O_2 system.

Table S1. Performance comparison of our method with previous PPi-based fluorescent approaches for ALP detection.

Principle	Linear range ($U\ L^{-1}$)	LOD ($U\ L^{-1}$)	Detection time (min)	Ref.
PPi-triggered competitive displacement of fluorescein-labeled DNA from MVCM	2~100	0.18	30~40	1
Copper-mediated DNA-sca□olded silver nanocluster switching	30~240	5	130~140	2
Inhibition of DNA-templated copper nanoparticles by PPi	0.3~7.5	0.3	70~80	3
Quenching and restoration of the fluorescence of CDs	2.5~40	1	120~130	4
PPi-mediated regulation of the fluorescence of CQDs	16.7~782.6	1.1	30~40	5
Inhibition of DNA-templated silver nanoclusters by PPi	0.1~250	0.078	85~95	6
Bifunctional MIL-53(Fe) with PPi-mediated peroxidase-like activity and oxidation-stimulated fluorescence switching	2~80	0.7	110~120	This work

References

1. C. H. Wang, G. E. Tang and H. L. Tan, *J. Mater. Chem. B*, 2018, **6**, 7614-7620.
2. J. L. Ma, B. C. Yin, X. Wu and B. C. Ye, *Anal. Chem.*, 2016, **88**, 9219-9225.
3. L. L. Zhang, J. J. Zhao, M. Duan, H. Zhang, J. H. Jiang and R. Q. Yu, *Anal.*

Chem., 2013, **85**, 3797-3801.

4. W. J. Kang, Y. Y. Ding, H. Zhou, Q. Y. Liao, X. Yang, Y. G. Yang, J. S. Jiang and M. H. Yang, *Microchim. Acta*, 2015, **182**, 1161-1167.
5. Z. S. Qian, L. J. Chai, Y. Y. Huang, C. Tang, J. J. Shen, J. R. Chen and H. Feng, *Biosens. Bioelectron.*, 2015, **68**, 675-680.
6. L. Y. Guo, D. L. Chen, M. H. Yang, *Microchim. Acta*, 2017, **184**, 2165-2170.